Band-edge photoluminescence and reflectivity of nonpolar $(11\bar{2}0)$ and semipolar $(11\bar{2}2)$ GaN formed by epitaxial lateral overgrowth on sapphire

T. Gühne,[1,*] Z. Bougrioua,[1,†] S. Laügt,[1] M. Nemoz,[1] P. Vennéguès,[1] B. Vinter,[1,2] and M. Leroux[1]
[1]*Centre de Recherche sur l'Hétéro-Epitaxie et ses Applications, Centre National de la Recherche Scientifique (CRHEA-CNRS), Rue B. Grégory, 06560 Valbonne, France*
[2]*Département de Physique, Université de Nice, Parc Valrose, 06130 Nice, France*
(Received 8 September 2007; published 8 February 2008)

Coalesced nonpolar $(11\bar{2}0)$ and semipolar $(11\bar{2}2)$ GaN layers obtained by epitaxial lateral overgrowth on sapphire have been studied by photoluminescence and reflectivity under normal incidence as a function of temperature and light polarization. In nonpolar GaN, two strongly allowed excitonic levels *A* and *C* are evidenced by reflectivity and are also observed in the luminescence spectra. The third exciton level (*B*) is only observed in the luminescence spectra, showing that its oscillator strength is mainly concentrated in transitions involving light polarized along the growth axis. The lower energy *A* exciton state is allowed for light polarized perpendicularly to the *c* axis. Therefore, for light polarized along the *c* axis, the thermal quenching of the luminescence of *A* results in a strong increase of the higher energy exciton emission, with an activation energy corresponding to their energetic separation. We observe a similar temperature induced increase of luminescence for transitions involving basal stacking faults and donor-acceptor pairs. In the latter case, our observation is evidence of an acceptor excited state due to the valence band splitting. Careful examination of the energy differences between the *A* exciton luminescence spectra recorded in both polarizations leads to an exchange splitting of 1 ± 0.5 meV, in good agreement with previous determinations. Our experimental results, exciton energies, and oscillator strengths are in good agreement with those calculated from a $\mathbf{k}=\mathbf{0}$ strained wurtzite valence band Hamiltonian using strain values measured by x-ray diffraction. Finally, the results for semipolar GaN are qualitatively similar to those obtained from nonpolar GaN. However, the optical selection rules are not as severe, owing to the fact that normal incidence light is never fully polarized perpendicular to the wurtzite basal plane.

DOI: 10.1103/PhysRevB.77.075308 PACS number(s): 71.20.Nr, 78.55.Cr, 71.55.Eq, 71.70.Gm

INTRODUCTION

After the spectacular breakthrough of the group III nitrides in the field of visible and UV optoelectronics in the early 1990s,[1] a current field of interest is their growth along directions different from the wurtzite *c* axis,[2–5] i.e., the growth of so-called nonpolar or semipolar nitrides. Indeed, most nitride devices are grown along the *c* axis, and it is known that huge polarization (piezoelectric and spontaneous) gradients are then present at nitride heterointerfaces.[6–9] In quantum wells, the induced Stark effect redshifts the transition energies but also strongly increases the ground state radiative lifetime in the case of wide wells and large electric field values (i.e., large differences in well-barrier materials). This is unfortunately the case as one goes from the blue wavelength range to the green or even yellow ones, where the human eye sensitivity is strongest. In an emitting device, increasing the radiative lifetime evidently favors nonradiative recombination, and the subsequent heating of the device active region is deleterious for its lifetime. In the framework of solid state lighting, the light emitting diode lifetime is a parameter of paramount importance for the profitability (counted in joules) of these epitaxial monocrystalline devices relative to simpler glass based ones as Edison's incandescent bulb or Auer's fluorescent tube. This motivates the research on device crystalline orientations that decrease or even annihilate interfacial polarization discontinuities in order to decrease the Stark effect. Another interest in the use of nonpolar or semipolar orientations with regard to the UV range is that above an Al composition around 0.2 in $Al_xGa_{1-x}N$, the valence band maximum symmetry is Γ_7 and the progressive transfer of the ground state oscillator strength to Γ_1 excitons with increasing *x* does not favor surface emission in *c*-oriented devices.[10,11]

These are strong stimulations for exploring the growth of nitride-based devices along nonpolar or semipolar orientations. However, heteroepitaxy on sapphire or other substrates results in large densities of structural defects, mainly basal stacking faults (BSFs) and threading dislocations.[2,5,12] Only recently have nice characteristics of light emitting diodes and laser diodes on nonpolar or semipolar GaN appeared. The latter results were obtained from structures grown on single crystal GaN slices cut along the desired orientation from thick freestanding *c*-plane GaN grown by hydride vapor phase epitaxy.[3,4] Such substrates are expensive and of limited size. A promising alternative would be to get large, low defect density nonpolar and semipolar GaN substrates by using epitaxial lateral overgrowth (ELO). ELO has proven to be an effective defect filtration means in conventional *c*-plane GaN epitaxy[13] and recent studies have shown that it is also the case for nonpolar and semipolar GaN epitaxy.[2,5]

In the present work, the optical properties of nonpolar and semipolar GaN grown by ELO on sapphire substrates are studied by luminescence and reflectivity as a function of temperature and light polarization.

EXPERIMENTAL DETAILS

A dielectric mask is deposited on nonpolar $(11\bar{2}0)$ or semipolar $(11\bar{2}2)$ GaN templates grown by metalorganic vapor phase epitaxy on $(1\bar{1}02)$ or $(10\bar{1}0)$ sapphire, respectively.[2,5] Stripes (2 or 3 μm) perpendicular to the c axis were opened in these masks; then, the growth was carried over by ELO up to coalescence of the overgrown stripes (3 or 7 μm) and the obtainment of planar surfaces.[5] The surface ratio of the laterally overgrown materials (the wings) to that of the materials directly grown above the mask openings (the seeds) is 60/40 to 70/30. The overall thickness of the samples is bigger than 5 μm. Thanks to the lateral overgrowth, the BSF densities are reduced to 5×10^3 cm^{-1} in the wings of semipolar GaN compared to some 10^5 cm^{-1} in the seeds (1.5×10^4 cm^{-1} compared to about 10^6 cm^{-1} in the nonpolar GaN case).[14] High resolution x-ray ($\lambda=0.154\,056$ nm) diffraction measurements were carried out in a Seifert XRD 3003 PTS-HR system, with a Ge(220) four-bounce monochromator and a 2 mm slit in front of the detector. For nonpolar GaN, the out-of-plane lattice parameter was more precisely measured using a Ge(220) two-bounce analyzer in front of the detector.

Nonspatially resolved photoluminescence (PL) and reflectivity experiments were performed in the 10–300 K range under normal incidence with an external f number of 1/10 and a spot size of several hundred micrometers. The spectral resolution was about 8000 for luminescence measurements and 1100 for reflectivity. Luminescence was excited either by the 325 nm line of a HeCd laser or the 244 nm line of a frequency-doubled Ar laser ($I_{max}\sim20$ W/cm^2). Reflectivity spectra were recorded by shining white light from a halogen bulb on the samples. The linear polarization of the emitted or reflected light was studied using a calcite Glan-Thomson prism.

RESULTS: NONPOLAR GaN

Figure 1 shows the reflectivity and luminescence spectra at 10 K of a nonpolar $(11\bar{2}0)$ oriented ELO GaN sample for light polarized along the c axis (hereafter the z direction, see inset in Fig. 1) or perpendicular to it (hereafter the y direction). Two pronounced excitonic reflectivity structures are recorded, one for each polarization. The ground state (A), at 3.476 ± 0.001 eV, is strongly allowed for light polarized along the y direction. Another excitonic level (C) is observed at higher energy (3.511 ± 0.001 eV) for light polarized along z. It is worth emphasizing that thanks to the improved structural quality of the wings of our ELO sample, these transitions are detected by simple reflectivity and not modulated reflectivity, as usually done in the case of heteroepitaxial nonpolar GaN on sapphire, SiC, or $LiAlO_2$.[15,16] The signal to noise ratio of the reflectivity spectra in Fig. 1 is about 5. Then, the absence of the A exciton (the C exciton) on the $E\|c$ spectrum (the $E\perp c$ spectrum) shows that its oscillator strength for light polarized along c (perpendicular to c) should be less than 20% of its total strength. A third wurtzite exciton, B, is not observed in Fig. 1 and is then expected to be mainly active for light polarized along the x direction in virtue of the sum rule.

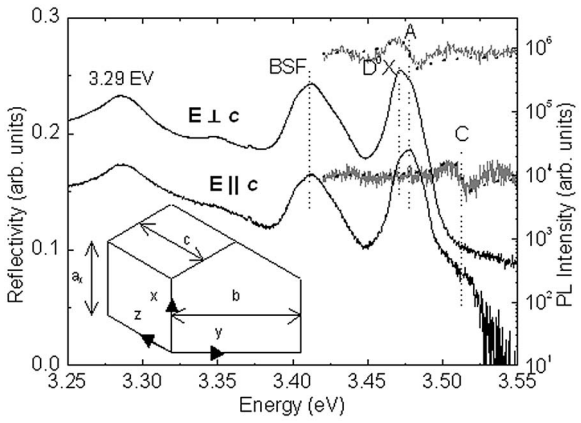

FIG. 1. Polarized reflectivity (linear scale) and photoluminescence (logarithmic scale) spectra of nonpolar $(11\bar{2}0)$ ELO GaN at 10 K. Light is polarized either perpendicular to the c axis (upper spectra) or parallel to it (lower spectra). The reflectivity spectra have been vertically shifted for clarity and the dashed lines are the calculated reflectivities. The luminescence scale is common for both polarizations. The inset defines the orthorhombic cell and the choice of axis used.

A factor of ~10 between the PL intensities recorded for $E\perp c$ and for $E\|c$, which is in agreement with the previous estimates of relative oscillator strengths, is measured in Fig. 1. These PL spectra are dominated by band-edge transitions involving free A excitons and donor bound excitons (D^0X) 6 meV lower in energy, as usual in the low temperature (T) spectra of undoped GaN.[17] Note a shoulder near 3.51 eV corresponding to the C exciton observed by reflectivity on the $E\|c$ PL spectrum. A very intense transition of composite nature is also observed at 3.41 eV. This PL band has been attributed to excitons bound to I_1-type BSFs.[14,18,19] Other PL transitions recorded in Fig. 1 are bands at 3.35 and 3.29 eV. Liu *et al.*,[19] in a combined transmission electron microscopy and cathodoluminescence (CL) study, tentatively attributed these two transitions to luminescence from prismatic stacking faults and partial dislocations, respectively, both defects terminating basal stacking faults. However, our previous CL study of nonpolar and semipolar ELO GaN (Ref. 14) has shown that though these lines are related to basal stacking faults, they can be recorded from regions where prismatic stacking faults and partial dislocations are absent.

Figure 2 displays the excitation power dependence of the 10 K PL spectra. It is seen that as the excitation power decreases, the 3.29 eV line shows a significant redshift, which has been attributed to a donor-acceptor pair (DAP)-like behavior.[20] Figure 2 also shows that as the excitation power decreases, the Huang-Rhys factor (estimated from the first LO phonon replica) of the 3.29 eV band increases from ~0.2 to 0.5, while its energy has decreased to 3.27 eV. The latter values are very near those of the usual residual acceptor-donor pair band in GaN. We conclude that in the case of our sample, the 3.29 eV band is in fact a superposition of a defect related transition at 3.29 eV and of the usual GaN DAP band near 3.27 eV.

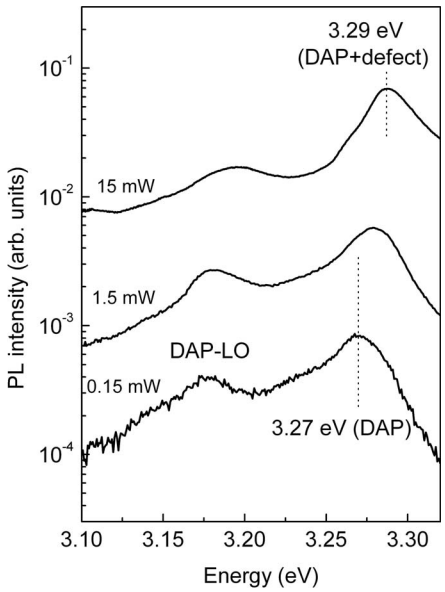

FIG. 2. Excitation power dependence of the 10 K photoluminescence of nonpolar $(11\bar{2}0)$ ELO GaN in the range of DAP transitions.

Figures 3(a) and 3(b) show the variation with temperature of the PL spectra of nonpolar ELO GaN for light polarized perpendicular and parallel to the c axis, respectively. It is seen in these figures that the defect related bands at 3.29, 3.35, and 3.41 eV quench rapidly with increasing temperature, as previously reported.[17,20,21] A striking feature in Fig. 3(b) relative to Fig. 3(a), apart from the lower overall PL efficiencies, is the emergence in the 60–120 K range of two high energy PL bands at 3.49 eV (labeled B) and 3.51 eV, the last one corresponding to the C exciton reported in Fig. 1. These transitions are hardly observed in Fig. 3(a) due to the unfavorable selection rules and to the predominant A exciton luminescence, strongly allowed for $E \perp c$.

The quenching in the 10–180 K range of the various transitions observed in Fig. 3 is reported as Arrhenius plots in Figs. 4(a) and 4(b), again for both light polarizations. For simplicity, the transitions are gathered into three groups, corresponding to the band-edge (BE) excitons (D^0X,A,B,C), the BSF-related band at 3.41 eV, and the 3.29 eV band which also includes the DAP band (and electron to acceptor transitions at high T). The weakness of the 3.35 eV band prevented any study of the T dependence of its intensity.

In Fig. 4(a), corresponding to $E \perp c$, the intensity quenching of the various transitions are fitted using either one or two thermally activated nonradiative recombination channels for each group,[17] i.e., respectively:

$$I = \frac{I_0}{(1 + a_1 \exp(-E_1/kT))} \tag{1a}$$

or

$$I = \frac{I_0}{(1 + a_1 \exp(-E_1/kT) + a_2 \exp(-E_2/kT))}. \tag{1b}$$

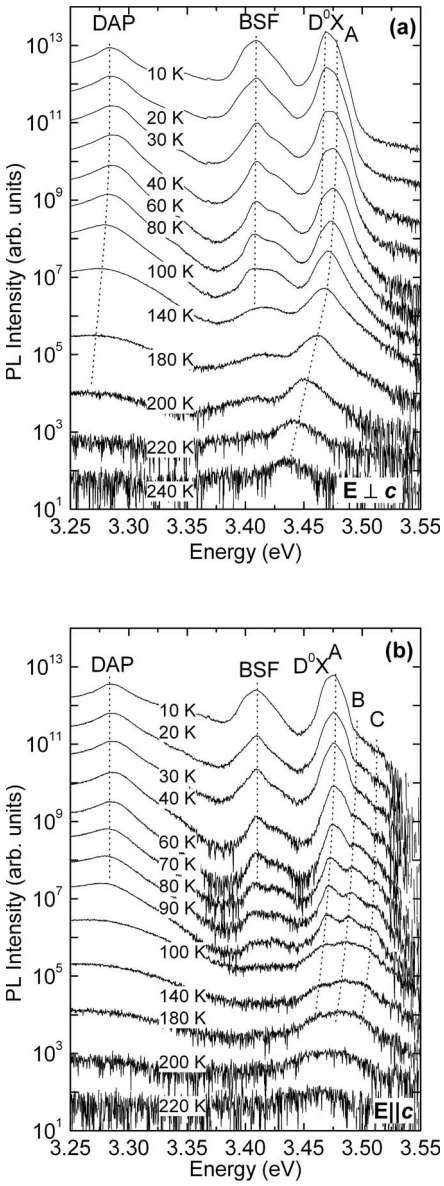

FIG. 3. Temperature dependent PL spectra of nonpolar $(11\bar{2}0)$ ELO GaN for light polarized perpendicular to the c axis (a) or parallel to it (b). The spectra have been vertically shifted for clarity.

The fitting of the intensity of the DAP band was done by considering that this band is the sum of a defect related transition and a DAP band, as evidenced in Fig. 2. The fitting curve of its intensity is then given by the sum of two equations [Eq. (1a)], a rapidly quenching one ($E_1 \sim 5$ meV) corresponding to the defect band supposed to be totally quenched above 100 K and a second one corresponding to the DAP, with a typical quenching activation energy of 185 ± 15 meV corresponding to hole release from the acceptors.[17,21,22]

The quenching of the band-edge exciton PL intensity is fitted using Eq. (1b) with activation energies $E_1 \sim 8 \pm 1$ meV and $E_2 \sim 100$ meV. The first low activation energy is likely to correspond to the thermal detrapping of donor bound excitons.[17] However, the second one is larger than those usually observed in polar (c-plane) heteroepitaxial

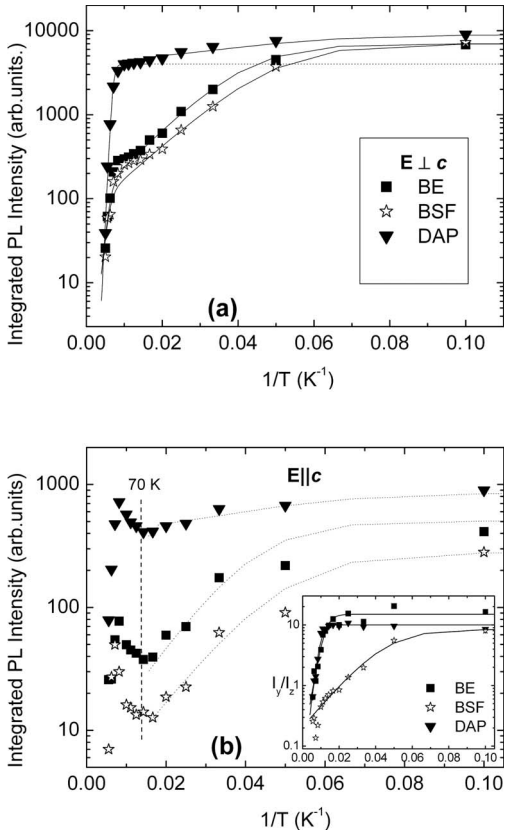

FIG. 4. Arrhenius plots of the temperature dependent PL intensities of BE excitons, BSF-related band, and DAP band in nonpolar $(11\bar{2}0)$ ELO GaN. Light is polarized perpendicular to the c axis (a) or parallel to it (b) and the intensity scales are common. The solid lines in (a) are fits with Eq. (1a) or (1b). The dotted lines in (b) are the fits of (a) in the 10–60 K range, vertically shifted for matching. The inset in (b) shows Arrhenius plots of the PL intensity ratios of the BE, BSF, and DAP bands between light polarized perpendicular to the c axis or parallel to it. The solid lines in this inset are fits using Eq. (1a).

GaN.[17] For the BSF-related band at 3.41 eV, Eq. (1b) is also used, with activation energies $E_1 \sim 8 \pm 1$ meV and $E_2 \sim 100$ meV. The E_1 value we find for the quenching of the 3.41 eV band is in excellent agreement with a similar study of a-plane GaN on sapphire by Paskov *et al.*[20] This first activation energy should correspond to hole detrapping when regarding basal stacking faults as type II cubic GaN quantum wells in a wurtzite GaN matrix that bind excitons.[18,20] However, since we find the same E_1 value for band-edge excitons and the 3.41 eV band, another possibility could be that the BSF-related quantum well excitons are also bound to donor impurities at low temperature. Finally, it is to be noted in Fig. 4(a) that in the 80–110 K temperature range, a small bump is observed in the PL quenching of the band-edge exciton PL and of the BSF-related PL. This could be due to hole release from the acceptors toward the bands[17,21] or also to the quenching of the 3.29 eV defect band.

In Fig. 4(b), we plot the PL intensity Arrhenius plots of the same transition observed for light polarized in the z direction (parallel to the c axis). Note that the intensity scales of Figs. 4(a) and 4(b) are the same. Up to ~70 K, the various transition intensities decrease in a way similar to the one observed for the other light polarization, as shown by the dotted curves corresponding to the fits in Fig. 4(a), vertically shifted. However, a salient feature in Fig. 4(b) is that, above 70 K, the PL intensities of these three groups of transitions show a strong increase with increasing T. This increase is further emphasized in the inset of Fig. 4(b), giving Arrhenius plots of the ratio of intensities measured for light polarized along y to that measured for light polarized along z. Simple considerations may explain this increase. Consider, for instance, the group of band-edge exciton lines. This group includes A, B, and C free excitons and donor bound excitons involving an A-type hole (D^0X in Fig. 1). For light polarized along z, the intensity is proportional to

$$I_z \propto \frac{n_{DX}}{\tau_{DXz}} + \frac{n_A}{\tau_{Az}} + \frac{n_B}{\tau_{Bz}} + \frac{n_C}{\tau_{Cz}}, \tag{2a}$$

and for light polarized along y, it is proportional to

$$I_y \propto \frac{n_{DX}}{\tau_{DXy}} + \frac{n_A}{\tau_{Ay}} + \frac{n_B}{\tau_{By}} + \frac{n_C}{\tau_{Cy}}, \tag{2b}$$

where n_A ($n_B, \ldots$) is the density of A excitons (B excitons etc.) and τ_{Az} ($\tau_{Ay}, \ldots$) is the hypothetical radiative lifetime of A excitons for emission of z-polarized (y-polarized) photons. From the reflectivity spectra in Fig. 1, we can anticipate that τ_{By} and $\tau_{Bz} \gg \tau_{Ay}$ and τ_{Cz}. We can also group the donor bound exciton line (D^0X) with that of the A exciton line (noting also that the D^0X line quenches rapidly with temperature,[17] as seen in Fig. 3). Within this rough two level model, the ratio of band-edge luminescence for both light polarizations reduces to

$$I_z/I_y \approx \frac{\left(\frac{n_A}{\tau_{Az}} + \frac{n_C}{\tau_{Cz}}\right)}{\left(\frac{n_A}{\tau_{Ay}} + \frac{n_C}{\tau_{Cy}}\right)} \approx \frac{\left(\frac{n_A}{\tau_{Az}} + \frac{n_C}{\tau_{Cz}}\right)}{\left(\frac{n_A}{\tau_{Ay}}\right)}. \tag{3}$$

Using $n_A/n_C = (N_A/N_C)\exp(E_{AC}/kT)$, i.e., assuming nondegenerate statistics, where N_A and N_C are effective densities of states and E_{AC} is the energy difference between A and C valleys, leads to

$$I_z/I_y \approx \left(\frac{\tau_{Ay}}{\tau_{Az}}\right)\left[1 + \left(\frac{N_C\tau_{Az}}{N_A\tau_{Cz}}\right)\exp\left(\frac{-E_{AC}}{kT}\right)\right]. \tag{4}$$

This means that the ratio I_y/I_z can be described by Eq. (1a). The corresponding fits to the ratios I_y/I_z are given in the inset of Fig. 4(b). In the case of the group of band-edge excitons, the activation energy deduced is 35 ± 4 meV, in very good agreement with the A-C energy separation of 33 meV obtained from Figs. 1 and 3. The increase of PL efficiency with increasing temperature for light polarized along the c axis is due to the thermal population of C valleys, which concentrates most of the $E \| c$ oscillator strength. In the case of the stacking fault related band at 3.41 eV, the activation energy deduced is lower (7 meV). We have no clear interpretation for this value, probably related to the complicated valence band structure of the wurtzite-cubic interface to which holes are bound.[18]

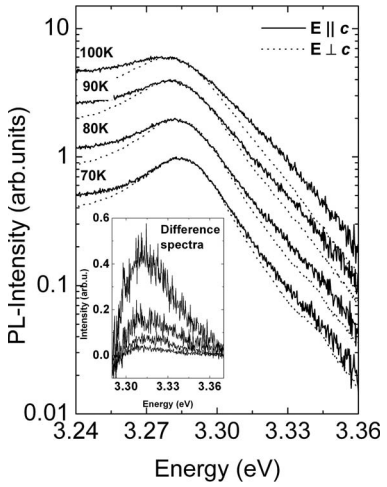

FIG. 5. PL spectra of nonpolar $(11\bar{2}0)$ ELO GaN around the maxima of the DAP band in the 70–100 K range for both light polarizations. The spectra are normalized to their maximum intensity, and the inset shows the difference spectra.

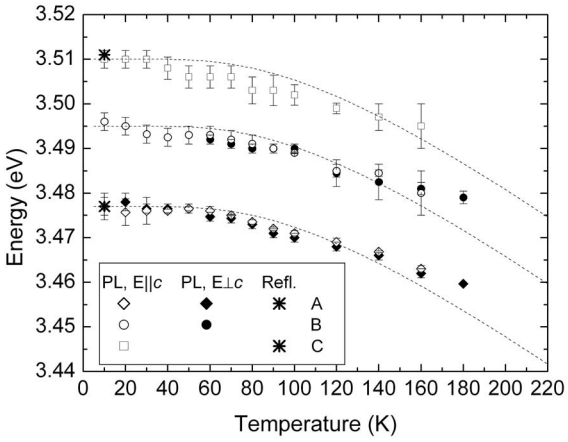

FIG. 6. Temperature dependence of the PL maxima of A, B, and C excitons of nonpolar $(11\bar{2}0)$ ELO GaN for both light polarizations. 10 K reflectivity data are also included. The dotted lines show the temperature dependence the excitonic gaps of c-plane GaN on sapphire.

Interestingly, we also note a strong increase with temperature ($T>70$ K) of the DAP band intensity for light polarized along the c axis, with an activation energy of 50 ± 10 meV, in Fig. 4(b). Since this band involves acceptor bound holes (should the band be of donor-acceptor pairs or electron to acceptor nature), an explanation should be that we are thermally populating an acceptor state linked to the C valleys. As an argument in favor of this explanation, we show the DAP band spectra for both polarizations in the 70–100 K range, normalized to their maximum intensity, in Fig. 5. Indeed, one observes the emergence of an additional band on the high energy side of the DAP band on the $E\|c$ spectra. The inset in Fig. 5 shows the difference between these normalized spectra. The additional band peaks near 3.315 eV, about 35 meV above the DAP band recorded for $E\perp c$. This energy separation is of the same order as the A-C separation and the activation energy obtained from Fig. 4(b). Though obtained in an indirect way, this is an experimental detection of acceptor excited states in GaN. The knowledge of the properties of these excited states is of importance, for instance, for interpreting the temperature dependent Hall effect in p-type GaN.

Finally, Figs. 6 and 7 are further evidences of the thermal population of higher energy exciton levels. The low intensity of the ground state PL due to the experimental geometry in Fig. 3(b) allows the resolution of two higher energy transitions, particularly in the 60–140 K temperature range. The higher energy one corresponds to the C exciton observed in reflectivity. We ascribe the second one to another free exciton level (B), since it is observed in a T range where shallow impurity-bound excitons are quenched. The contribution of the various transitions in the band-edge excitonic band has been estimated by deconvolution of the spectra in Figs. 3(a) and 3(b). The energy separation between the three free exciton levels is nearly temperature independent, as shown in Fig. 6, which compares the T dependence of the A, B, and C exciton energies with that of c-plane GaN on sapphire.[23] Above 140 K, the excitonic gaps decrease less steeply than in the case of c-plane GaN. However, our results are in good agreement with a previous determination of the T dependence of gaps of nonpolar GaN on sapphire.[20]

Figure 7 displays Arrhenius plots of the intensity ratios of A and B or C PL bands for both polarizations. Following the previous discussion, fits were done using Eq. (1). In the case of light polarized perpendicularly to the c axis, the activation energy for thermal population of B is found to be 16 ± 3 meV, in good agreement with the separation deduced from the PL spectra, i.e., 18 ± 2 meV. For light polarized parallel to c, the activation energy for C population is 30 ± 5 meV, again in good agreement with the A-C separation. However, the fit to the B exciton intensity in this geometry is poor, presumably due to the difficulty in the deconvolution of a weak transition located between two higher intensity ones.

RESULTS: SEMIPOLAR GaN

This long presentation of the luminescence and reflectivity of nonpolar $(11\bar{2}0)$ ELO GaN will help us present the

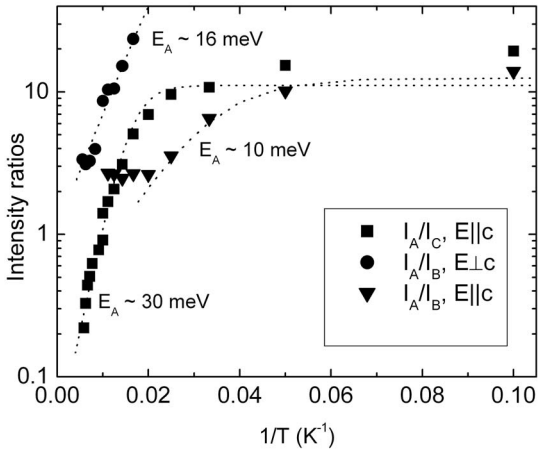

FIG. 7. Arrhenius plots of the ratios of A and B or C exciton PL intensities of nonpolar $(11\bar{2}0)$ ELO GaN for both light polarizations. The solid lines are fits using Eq. (1a).

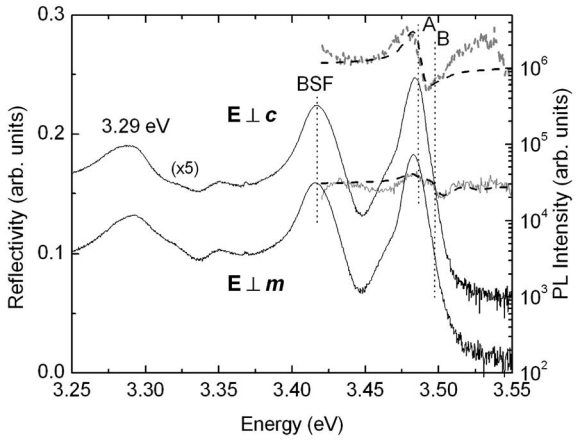

FIG. 8. Luminescence (logarithmic scale) and reflectivity (linear scale) spectra at 10 K of semipolar $(11\bar{2}2)$ ELO GaN for light polarized $\perp c$ (upper spectra) or $\perp m$ (lower spectra). The reflectivity spectra have been vertically shifted for clarity and the dashed lines are calculated reflectivities. Note the five times multiplying factor of the upper PL spectrum.

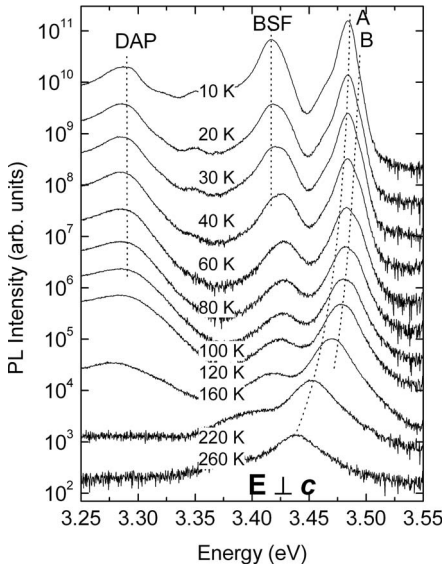

FIG. 9. Temperature dependent PL spectra of semipolar $(11\bar{2}2)$ ELO GaN for light polarized $\perp c$. The spectra have been vertically shifted for clarity.

properties of semipolar $(11\bar{2}2)$ ELO GaN in a shorter way. As Fig. 1 in the case of nonpolar GaN, Fig. 8 shows the 10 K reflectivity and PL spectra of semipolar GaN for light polarized perpendicular to the c axis, i.e., parallel to the $(1\bar{1}00)$ axis (or m axis), or parallel to the projection of the c axis, i.e., perpendicular to the m axis. We use this expression $(E \perp m)$ in the following.

For $E \perp m$, two excitonic reflectivity structures are clearly resolved, at 3.4865 eV (A) and 3.497 eV (B). For $E \perp c$, one strong excitonic reflectivity feature is recorded, interestingly about 1 meV lower in energy than A in the other geometry, at 3.4855 eV. In this polarization, the B exciton can also be observed as a shoulder on the A exciton feature. The PL spectra are similar to those of nonpolar GaN. The PL peak energy is slightly lower than the excitonic one given by reflectivity due to the unresolved contribution of donor bound excitons in the low temperature PL spectra. Transitions from basal stacking faults and other defects at 3.42, 3.35, and 3.29 eV are also observed. However, while there was a ratio of about 10 in the band-edge PL intensities recorded for both polarizations in the case of nonpolar GaN (see Fig. 1), there is now only a ratio of 2 between the band-edge PL intensities recorded for $E \perp c$ and $E \perp m$. This is obviously due to the fact that in semipolar GaN under normal incidence, light cannot be polarized perpendicular to both the x and y directions of the wurtzite structure,[24] as defined in the inset of Fig. 1.

Figure 9 shows the T-dependent PL spectra of semipolar ELO GaN recorded for light polarized perpendicular to c $(\|m)$. This temperature dependence is very similar to the one shown in Fig. 3(a) in the case of nonpolar GaN. However, with increasing temperature, the contribution of B excitons to the spectra is clearly observed, in agreement with its observation on the reflectivity spectra of Fig. 8. We do not show the T-dependent PL spectra recorded for the other polarization, since they are similar to those shown in Fig. 9, apart from the previously mentioned difference in intensity. Indeed, since the A and B excitons cannot be extinguished under normal incidence in the case of semipolar GaN, the ground state A exciton always dominates the band-edge luminescence, contrary to the case of nonpolar ELO GaN, where the ground state extinction allows us to clearly discriminate B and C excitons [Fig. 3(b)].

DISCUSSION

Strong anisotropic effects have been observed in this work, particularly in the case of nonpolar GaN, and these effects are also observed in the wurtzite basal plane, evidencing a lowering of the crystal symmetry.

The in-plane and out-of-plane lattice parameters of nonpolar ELO GaN were measured by x-ray diffraction. This analysis showed that the wurtzite cell is deformed to an orthorhombic one (actually slightly monoclinic) with parameters $a_x = 3.1922 \pm 0.0005$ Å, $b = 5.510 \pm 0.001$ Å, and $c = 5.182 \pm 0.001$ Å (see the inset in Fig. 1). These values have to be compared with those measured by Tsuda *et al.*[25] on a metallorganic chemical vapor deposition (MOCVD)-grown a-plane GaN template on r-plane sapphire: $a_x = 3.194$ Å, $b = 5.504$ Å, and $c = 5.170$ Å. Our sample is less compressed in plane and less extended out of plane. This is related to the ELO growth and, actually, x-ray diffraction gives average lattice parameters, which include template, seeds, and wings of our sample. Using $a_0 = 3.189$ Å and $c_0 = 5.185$ Å for relaxed GaN gives the following strain values: $\varepsilon_{xx} = \varepsilon_1 = (1.0 \pm 0.2) \times 10^{-3}$, $\varepsilon_{yy} = \varepsilon_2 = (-2.5 \pm 0.2) \times 10^{-3}$, and $\varepsilon_{zz} = \varepsilon_3 = (-0.6 \pm 0.2) \times 10^{-3}$ [where we have introduced Voigt's notation and used $\varepsilon_2 = (b - a_0\sqrt{3})/a_0\sqrt{3}$].

Estimating the out-of-plane stress in our sample gives $\sigma_1 = C_{11}\varepsilon_1 + C_{12}\varepsilon_2 + C_{13}\varepsilon_3 = -0.036 \pm 0.13$ GPa using $C_{11} = 390$ GPa, $C_{12} = 145$ GPa, $C_{13} = 106$ GPa, and C_{33}

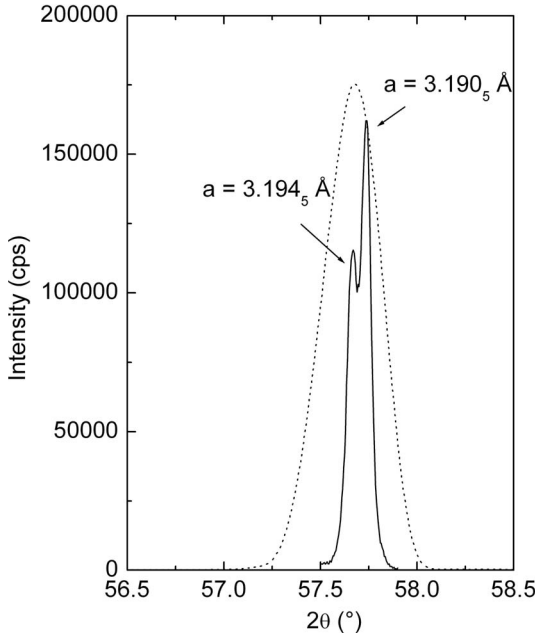

FIG. 10. Low (dotted line) and high resolution (solid line) x-ray diffraction patterns of $(11\bar{2}0)$ planes of nonpolar $(11\bar{2}0)$ ELO GaN.

=398 GPa.[26] This is in agreement with the condition $\sigma_1=0$ usually assumed in the case of strained heteroepitaxy.

In the next step, we measured the out-of-plane lattice parameter a_x of nonpolar ELO GaN by high resolution x-ray diffraction (for geometrical reasons, the other lattice parameters cannot be measured that way). Figure 10 shows the corresponding low and high resolution diffractograms. A double peak can be seen, corresponding to two lattice parameter values: 3.1945 and 3.1905 Å. Since one of these values is very near that measured by Tsuda *et al.*[25] for GaN on *r*-plane sapphire and since the intensity ratio of both peaks in Fig. 10 is ~1.3, it is tempting to attribute the two peaks in the high resolution diffraction pattern of Fig. 10 to diffraction from the seeds (low angle peak) and wings (high angle peak) of our ELO sample.

Our previous CL study[14] has shown that the seed region has a much lower radiative efficiency than the wing one and, in particular, no excitonic emission. Then, in order to interpret the energies and oscillator strengths of the excitonic transitions observed in the present study, we need to know the strain tensor of the wings of our sample.

We already know that the average strain in our sample obeys $\sigma_1=0$ within uncertainty bars. To obtain the missing strain values of the ELO wings (ε_{iw}), we use the fact that they grow freely in the z directions also during ELO. Using the system $\sigma_1=0$, $\sigma_3=0$, and $\varepsilon_{1w}=(0.5\pm0.2)\times10^{-3}$ (from the data in Fig. 10), we obtain $\varepsilon_{2w}=(-1\pm0.3)\times10^{-3}$ and $\varepsilon_{3w}=(0.3\pm0.2)\times10^{-3}$ in the wings of our sample.

Knowing the strain tensor, we have calculated the band structure at $\mathbf{k}=\mathbf{0}$ and the corresponding optical oscillator strengths using the strained wurtzite valence band Hamiltonian.[27,28] We use the same deformation potentials as Ghosh *et al.*,[15] who studied *m*-plane GaN grown on γ-$LiAlO_2$ by photoreflectance. However, we found it necessary to change the crystal field and spin-orbit coupling terms to $\Delta_1=13$ meV and $\Delta_2=\Delta_3=6$ meV, respectively. This, together with an unperturbed gap of 3.5215 eV, allowed us to reproduce the *A*, *B*, and *C* excitonic gaps of strain-free homoepitaxial GaN.[29] The deformation potential values also assure agreement with the value $dE_A/d\varepsilon_1=-9\pm0.5$ meV measured in biaxially strained *c*-plane GaN.[30,31] (Another set of deformation potentials was proposed by Alemu *et al.*[32] Their values are slightly different except for the shear deformation potential D_5 whose sign is reversed. This is due to an interchange of the definitions of the x and y directions, which is of no importance in C_{6v} symmetry but not in C_{2v} symmetry.)

We get a good agreement with our experimental results on ELO nonpolar GaN using $\varepsilon_{1w}=0.35\times10^{-3}$, $\varepsilon_{2w}=-1.33\times10^{-3}$, and $\varepsilon_{3w}=0.10\times10^{-3}$, within the quoted strain uncertainty bars. The three exciton energies and the repartition of their relative oscillator strengths f are

$$E_A=3.477\ \text{eV},\quad f_{Ay}=0.90,\quad f_{Ax}=0.07,$$

$$E_B=3.494\ \text{eV},\quad f_{Bx}=0.74,\quad f_{Bz}=0.24,$$

$$E_C=3.511\ \text{eV},\quad f_{Cx}=0.20,\quad f_{Cz}=0.74.$$

These calculated values confirm the experimentally observed behavior of the band-edge transitions. In reflectivity, only the *A* (*C*) exciton can be observed when light is polarized $E\perp c$ ($E\|c$). This is due to the too low oscillator strength in the opposite polarization. On the other hand, it also explains why the *B* exciton can only be observed in PL. The relatively strong oscillator strength in direction z ($f_{Bz}=0.24$) allows it to be observed in photoluminescence when the ground state PL is almost extinguished by the polarizer, but it is at the limit of observation by reflectivity within the dynamic range of the experiment.

The calculated reflectivity spectra, using a Gaussian broadened Lorentz oscillator model, are shown as dashed lines in Fig. 1. The fitting parameters are $E_A=3.476$ eV, $f_{Ay}=25\,000\pm3000$ meV^2, and $\sigma_A=8$ meV ($E\perp c$) and $E_C=3.511$ eV, $f_{Cz}=25\,000\pm3000$ meV^2, and $\sigma_C=8$ meV ($E\|c$), where σ is the Gaussian broadening of the transition.

The energies given by these fits are in good agreement with those determined by PL and the calculations. However, the oscillator strengths obtained are lower than those reported for the *A* exciton in *c*-plane GaN, which are in the 40 000–50 000 meV^2 range.[23,33,34] However, as we mentioned earlier, spatially resolved CL of nonpolar ELO GaN has shown that there is no band-edge excitonic PL from the seeds of our sample due to their much larger defect densities (stacking faults and partial dislocations) than the wings.[14] The apparent oscillator strengths of our sample should be multiplied by 1.67, which is the ratio of the total surface of the sample to the surface of the ELO wings when regarding the seeds as "dead" material for excitonic transitions. This greatly improves the agreement with the measured and expected oscillator strengths.

We shall not discuss the strain state of the semipolar ELO GaN sample. Strained heteroepitaxy in a direction that is not a principal axis of the strain tensor of wurtzite leads to non-

zero shear components of the strain[35] and the structure loses the symmetry. The higher ground state energy of semipolar ELO GaN relative to nonpolar ELO GaN shows that the former is more compressed than the latter.

We shall only briefly discuss the polarized reflectance spectra (shown in Fig. 8), taking into account our results for nonpolar GaN, i.e., the optical anisotropy in the basal plane. The dashed lines on the reflectance spectra in Fig. 8 are fits using a two or three Gaussian broadened Lorentz oscillator model. The fitting parameters are as follows. For $E \perp c$:

$$E_A = 3.4855 \text{ eV}, \quad f_{Ay} = 37\,000 \pm 3000 \text{ meV}^2, \quad \sigma_{Ay} = 6.5 \text{ meV}$$

and

$$E_B = 3.497 \text{ eV}, \quad f_{By} = 4000 \pm 2000 \text{ meV}^2, \quad \sigma_{By} = 6.5 \text{ meV}.$$

For $E \perp m$:

$$E_A = 3.4865 \text{ eV}, \quad f_A = 9000 \pm 2000 \text{ meV}^2, \quad \sigma_A = 6.5 \text{ meV},$$

$$E_B = 3.497 \text{ eV}, \quad f_B = 13\,000 \pm 2000 \text{ meV}^2, \quad \sigma_B = 6.5 \text{ meV},$$

and

$$E_C \approx 3.522 \text{ eV}, \quad f_C = 4000 \pm 2000 \text{ meV}^2, \quad \sigma_C = 6.5 \text{ meV}.$$

We first note that the ground state is mainly polarized along the y direction, as in the case of nonpolar GaN. Its oscillator strength of 37 000 meV^2 is in the range of values quoted for the A exciton in c-plane GaN. On the other hand, the oscillator strength of the B one is very low for this polarization. For light polarized perpendicular to the m direction, the ground state oscillator strength is $f_{Az}\cos^2(\theta) + f_{Ax}\sin^2(\theta)$ where θ is the angle between the c axis and the growth direction.[24] Since $\theta = 31.6°$ in undeformed GaN, we then estimate $0.73f_{Az} + 0.27f_{Ax} \approx 9000$ meV^2 and, for the B excitons, $0.73f_{Bz} + 0.27f_{Bx} \approx 13\,000$ meV^2. From these values and remembering that the optical oscillator strength of A excitons in unstrained GaN is in the 40 000–50 000 meV^2 range, we can estimate that $29\,000 \text{ meV}^2 \leqslant f_{Bx} \leqslant 45\,000 \text{ meV}^2$ and $0 \leqslant f_{Bz} \leqslant 7000 \text{ meV}^2$. Regarding the A exciton, the same assumptions point to a very weak oscillator strength for the electric field in the z direction ($f_{Az} \leqslant 1000 \text{ meV}^2$). As in the case of nonpolar ELO GaN, a strong optical anisotropy in the basal plane is observed in semipolar ELO GaN. A weak structure at 3.522 eV is observed on the $E \perp m$ reflectivity spectrum in Fig. 8. We tentatively attribute it to the third exciton C. However, its oscillator strength is very weak. We have no clear explanation for this fact at the moment, probably related to the circumstance that in this sample, the C exciton is resonant with the A and B valence band continuums.

Our previous transmission electron microscopy and cathodoluminescence studies have shown that the crystalline quality of semipolar GaN is higher than that of nonpolar GaN in the case of heteroepitaxy on sapphire, and this is valid for both wing and seed materials.[14] This improved quality manifests itself in the reflectivity spectra. In semipolar ELO GaN, the oscillator strengths of excitons are within the range of values measured in c-plane GaN (i.e., there is no need to regard the seeds as dead material). Moreover, the inhomogeneous broadening parameters σ are also lower in semipolar ELO GaN than in nonpolar.

Another point is to be emphasized. The fitting of the reflectivity spectra of semipolar ELO GaN (Fig. 8) has shown that there is a 1 ± 0.5 meV blueshift between the A exciton energy obtained for $E \perp c$ and that measured for $E \perp m$. Though we have not observed such a shift in the reflectivity spectra of nonpolar ELO GaN due to the poor signal to noise ratio (see Fig. 1), we note in that case a similar blueshift of 1 ± 0.5 meV of the A exciton PL energy between the two polarizations, in the temperature range of 60–140 K where the precision on the energy of A is maximum due to its intensity and the quenching of donor bound exciton PL. We think that these slight shifts are significant and reflect the excitonic electron-hole exchange splitting. Indeed, our previous calculations concerned electron-hole transitions and the exciton energies were obtained by subtracting the excitonic Rydberg ($\approx$26 meV for A, B, and C) from the calculated band-to-band transition energies. From an excitonic point of view, it is known that, in wurtzite symmetry, excitons formed from a Γ_7 electron and a Γ_9 hole from the A valence bands leads to two levels of Γ_5 and Γ_6 symmetries, the latter being dipole forbidden and the former being allowed for $E \perp c$ optical transitions. Excitons formed by Γ_7 electrons and Γ_7 holes from the B and C valence bands are split into Γ_1, Γ_5, and Γ_2 symmetries. Γ_1 excitons are allowed for $E \| c$ optical transitions and Γ_2 ones are dark.[32,36] Here, Γ_1 to Γ_9 label irreducible representations of the C_{6v} point group. Lowering the symmetry from C_{6v} to C_{2v} due to the anisotropic deformations in the basal plane, as observed in our samples, leads to the following splittings and selection rules:

$$\Gamma_1 \to \Gamma_1(z), \quad \Gamma_2 \to \Gamma_3(\text{dark}), \quad \Gamma_5 \to \Gamma_2(x) + \Gamma_4(y), \quad \Gamma_6 \to \Gamma_1(z) + \Gamma_3(\text{dark}),$$

where the Γ on the right of the arrows are now irreducible representations of the C_{2v} point group. The allowed polarizations for optical transitions within the dipole approximation are given in brackets. One can see first that in our samples, the transitions involving A excitons for z-polarized light (i.e., $E \| c$) originate from the Γ_6 state of A, which is dipole forbidden in wurtzite symmetry. It is then no surprise that in our samples, the corresponding oscillator strength f_{Az} is very weak. Second, the separation between the Γ_5 and Γ_6 levels of unstrained GaN is the exchange interaction parameter γ, with $\gamma = 0.6$ meV.[32,36] We then ascribe the 1 ± 0.5 meV blueshift of the PL of A excitons in nonpolar ELO GaN to the excitonic exchange interaction. A similar origin is given to the same splitting observed in the polarized reflectivity spectra of A excitons in semipolar ELO GaN. Our experimental resolution is unfortunately too poor to measure this splitting in the case of the B or C excitons.

In order to further evaluate the optoelectronic quality of nonpolar and semipolar ELO GaN, we compared their relative unpolarized PL intensities at 10 and 300 K with that of a standard *c*-oriented (polar) undoped MOCVD-grown GaN layer, with threading dislocations density in the low 10^8 cm^{-1}. The PL yield of the three samples, integrated from 1.8 to 3.6 eV (i.e., including yellow band, donor-acceptor pair band, etc.) are the same within a factor less than 2 at both 10 and 300 K. However, as expected, there are differences in the band-edge excitonic PL intensities. The ratios of band-edge PL intensities are 1/0.2/0.05 at 10 K and 1/0.9/0.15 at 300 K for the polar/semipolar/nonpolar samples, respectively. At 10 K, the decrease of band-edge PL yield in ELO nonpolar and semipolar GaN is compensated by hole trapping on acceptors and by exciton trapping on stacking faults, both effects preventing minority carriers from diffusing toward nonradiative centers. The larger acceptor doping in nonpolar and semipolar ELO GaN relative to *c*-oriented GaN, evidenced by the intensities of the DAP band, is tentatively attributed to silicon acceptors from the SiO_2 or SiN_x ELO masks used. The similar band-edge PL efficiencies of polar and semipolar ELO GaN at 300 K attest to the quality of the latter. The low structural defect densities in the wings of this sample, in particular, the absence of dislocations,[14] compensate the fact that these wings represent only 60% of the sample surface.

Finally, we point out that due to the anisotropic strain in the basal plane, the ground state oscillator strength is concentrated in transitions polarized along *y* (see inset in Fig. 1) in nonpolar and semipolar ELO GaN. For an edge emitting laser, this favors TE modes, since the corresponding oscillator strength is increased by almost a factor of 2 relative to unstrained GaN. In the case of homoepitaxial lasers grown on freestanding *m*-plane GaN, as those described in Refs. 3 and 4, the GaN is unstrained. However, the (Ga,In)N quantum wells, which are the lasers' active region, are anisotropically strained in the basal plane by epitaxy on GaN, and as such, their ground state should show the same beneficial enhancement of oscillator strength. This is another interest of the use of nonpolar or semipolar orientations for nitride optoelectronics.

CONCLUSIONS

Nonpolar $(11\bar{2}0)$ and semipolar $(11\bar{2}2)$ GaN grown by epitaxial lateral overgrowth on $(1\bar{1}02)$ or $(10\bar{1}0)$ sapphire, respectively, have been studied by polarization dependent reflectivity and luminescence under normal incidence. In both cases, the strain anisotropy in the basal plane leads to an excitonic ground state polarized along the $(1\bar{1}00)$ direction (the *m* axis). In the case of nonpolar GaN, this allows to almost completely extinguish this ground state by a suitable polarizer orientation, making possible the study of high energy transitions up to now unseen. This is, for instance, the case of luminescence from acceptor states linked to the upper *C* valence band. This example shows that though GaN is a wide band gap material, it is a well-behaved semiconductor in the framework of the hydrogenic approximation. With increasing temperature in the 10–300 K range, the thermal population of upper exciton states, also showing linear polarization, leads to an excitonic band almost unpolarized at room temperature. In spite of the broadening of optical transitions due to heteroepitaxy, the material quality is sufficient to allow the detection of fine structures such as the excitonic exchange splitting of the ground state. The presence of structural defects such as stacking faults or others still manifests itself through specific PL bands in the low temperature spectra.

ACKNOWLEDGMENTS

We are grateful to G. Nataf and C. Morhain for their help in this study. This work was supported by the *PARSEM* Marie Curie Research Training Network (MRTN-CT-2004-005583), funded by the European Community's Sixth Framework Program.

*Corresponding author: tg@crhea.cnrs.fr

†Present adress: IEMN, CNRS and Lille University, 59652 Villeneuve d'Ascq, France.

[1] S. Nakamura and G. Fasol, *The Blue Laser Diode* (Springer, Berlin, 1997).

[2] M. D. Craven, S. H. Lim, F. Wu, J. S. Speck, and S. P. DenBaars, Appl. Phys. Lett. **81**, 1201 (2002).

[3] K. Okamoto, H. Ohta, S. F. Chichibu, J. Ichihara, and H. Takasu, Jpn. J. Appl. Phys., Part 2 **46**, L187 (2007).

[4] M. C. Schmidt, K. C. Kim, R. M. Farrell, D. F. Feezell, D. A. Cohen, M. Saito, K. Fujito, J. S. Speck, S. P. Denbaars, and S. Nakamura, Jpn. J. Appl. Phys., Part 2 **46**, L190 (2007).

[5] Z. Bougrioua, M. Laügt, P. Vennéguès, I. Cestier, T. Gühne, E. Frayssinet, P. Gibart, and M. Leroux, Phys. Status Solidi A **204**, 282 (2007).

[6] T. Takeuchi, S. Sota, M. Katsuragawa, M. Komori, H. Takeuchi, H. Amano, and I. Akasaki, Jpn. J. Appl. Phys., Part 2 **36**, L382 (1997).

[7] J. S. Im, H. Kollmer, J. Off, A. Sohmer, F. Scholz, and A. Hangleiter, Phys. Rev. B **57**, R9435 (1998).

[8] M. Leroux, N. Grandjean, M. Laügt, J. Massies, B. Gil, P. Lefebvre, and P. Bigenwald, Phys. Rev. B **58**, R13371 (1998).

[9] P. Lefebvre, A. Morel, M. Gallart, T. Taliercio, J. Allègre, B. Gil, H. Mathieu, B. Damilano, N. Grandjean, and J. Massies, Appl. Phys. Lett. **78**, 1252 (2001).

[10] M. Leroux, S. Dalmasso, F. Natali, S. Hélin, C. Touzi, S. Laügt, M. Passerel, F. Omnès, F. Semond, J. Massies, and P. Gibart, Phys. Status Solidi B **234**, 887 (2002).

[11] M. Leroux, F. Semond, F. Natali, B. Damilano, A. Dussaigne, N. Grandjean, A. Le Louarn, S. Vézian, and J. Massies, Superlattices Microstruct. **36**, 659 (2004).

[12] P. Vennéguès, F. Mathal, and Z. Bougrioua, Phys. Status Solidi C

3, 1658 (2006).
[13] P. Gibart, Rep. Prog. Phys. **67**, 667 (2004).
[14] T. Gühne, Z. Bougrioua, P. Vennéguès, M. Leroux, and M. Albrecht, J. Appl. Phys. **101**, 113101 (2007).
[15] S. Ghosh, P. Waltereit, O. Brandt, H. T. Grahn, and K. H. Ploog, Phys. Rev. B **65**, 075202 (2002).
[16] P. Misra, U. Behn, O. Brandt, H. T. Grahn, B. Imer, S. Nakamura, S. P. DenBaars, and J. S. Speck, Appl. Phys. Lett. **88**, 161920 (2006).
[17] M. Leroux, N. Grandjean, B. Beaumont, G. Nataf, F. Semond, J. Massies, and P. Gibart, J. Appl. Phys. **86**, 3721 (1999).
[18] Y. T. Rebane, Y. G. Shreter, and M. Albrecht, Phys. Status Solidi A **164**, 141 (1997).
[19] R. Liu, A. Bell, F. A. Ponce, C. Q. Chen, J. W. Yang, and M. A. Khan, Appl. Phys. Lett. **86**, 021908 (2005).
[20] P. P. Paskov, R. Schilano, B. Monemar, T. Paskova, S. Figge, and D. Hommel, J. Appl. Phys. **98**, 093519 (2005).
[21] M. A. Reschikov and H. Morkoç, J. Appl. Phys. **97**, 061301 (2005).
[22] M. A. Reshchikov and R. Y. Korotkov, Phys. Rev. B **64**, 115205 (2001).
[23] L. Siozade, S. Collard, M. Mihailovic, J. Leymarie, A. Vasson, N. Grandjean, M. Leroux, and J. Massies, Jpn. J. Appl. Phys., Part 1 **39**, 20 (2000).
[24] B. Gil, Appl. Phys. Lett. **90**, 121903 (2007).
[25] M. Tsuda, H. Furukawa, A. Honshio, M. Iwaya, S. Kamiyama, H. Amano, and I. Akasaki, Phys. Status Solidi B **243**, 1524 (2006).
[26] A. Polian, M. Grimsdich, and I. Grzegory, J. Appl. Phys. **79**, 3343 (1996).
[27] M. Suzuki, T. Uenoyama, and A. Yanase, Phys. Rev. B **52**, 8132 (1995).
[28] S. L. Chuang and C. S. Chang, Phys. Rev. B **54**, 2491 (1996).
[29] K. P. Korona, A. Wysmolek, K. Pakula, R. Stiepnewski, J. M. Baranowski, I. Grzegory, B. Luznik, M. Wroblewski, and S. Porowski, Appl. Phys. Lett. **69**, 788 (1996).
[30] H. Lahrèche, M. Leroux, M. Laügt, M. Vaille, B. Beaumont, and P. Gibart, J. Appl. Phys. **87**, 577 (2000).
[31] M. Leroux, H. Lahrèche, F. Semond, M. Laügt, E. Feltin, B. Beaumont, P. Gibart, and J. Massies, Mater. Sci. Forum **353–356**, 795 (2001).
[32] A. Alemu, B. Gil, M. Julier, and S. Nakamura, Phys. Rev. B **57**, 3761 (1998).
[33] N. Antoine-Vincent, F. Natali, D. Byrne, A. Vasson, P. Disseix, J. Leymarie, M. Leroux, F. Semond, and J. Massies, Phys. Rev. B **68**, 153313 (2003).
[34] F. Semond, I. R. Sellers, F. Natali, D. Byrne, M. Leroux, J. Massies, N. Ollier, J. Leymarie, P. Disseix, and A. Vasson, Appl. Phys. Lett. **87**, 021102 (2005).
[35] A. E. Romanov, T. J. Baker, S. Nakamura, and J. S. Speck, J. Appl. Phys. **100**, 023522 (2006).
[36] M. Julier, J. Campo, B. Gil, J. P. Lascaray, and S. Nakamura, Phys. Rev. B **57**, R6791 (1998).